Published in final edited form as:
Nat Methods. 2009 October ; 6(10): 737–740. doi:10.1038/nmeth.1368.

Imaging of intracellular free Zn^{2+} in real time using genetically-encoded FRET sensors

Jan L. Vinkenborg[1], **Tamara J. Nicolson**[2], **Elisa A. Bellomo**[2], **Melissa S. Koay**[1], **Guy A. Rutter**[2,*], and **Maarten Merkx**[1,*]

[1]Laboratory of Chemical Biology, Department of Biomedical Engineering, Eindhoven University of Technology, Den Dolech 2, 5612AZ Eindhoven, The Netherlands [2]Section of Cell Biology, Division of Medicine, Imperial College London, Exhibition Road, South Kensington, SW72AZ, London, U.K.

Abstract

Whilst Zn^{2+} ions are critical regulators of many fundamental cellular processes, methods to monitor the free concentrations of these ions dynamically within living cells are presently limited. We have developed a series of genetically-encoded Förster Resonance Energy Transfer (FRET)-based sensors that display a large ratiometric change upon Zn^{2+} binding, have affinities that span the pico- to nanomolar range, and can readily be targeted to subcellular organelles. These sensors reveal that the free cytosolic Zn^{2+} concentration of fibroblasts and pancreatic islet β-cells is tightly buffered at ~400 pM, a level at least 10^3-fold lower than that in secretory granules.

Introduction

Transition metals pose an interesting dilemma for living organisms as they are essential cofactors for numerous enzymes and proteins, but at the same time very toxic in their free form1. Mechanisms to control this delicate balance may vary for different metal ions, and also between organisms. Copper homeostasis in eukaryotes has been shown to involve specific copper chaperone proteins that transfer Cu^{+} to various cellular targets without releasing it into the cytosol2. Similar chaperones have not been identified for Zn^{2+}; instead a general Zn^{2+} buffering mechanism has been proposed in which the free cytosolic Zn^{2+} concentration in mammalian cells is kept constant at pM-nM levels3,4. The free concentration of transition metal ions is also likely to differ substantially between subcellular locations, as mM concentrations of total Zn^{2+} have been reported for pancreatic β cell granules5 and inferred for secretory vesicles in neuronal6 and mast cells7.

Current knowledge of transition metal homeostasis is based mostly on *in vitro* biochemical characterization of its protein components such as metal importers and exporters,

*Correspondence should be addressed to G.A.R (g.rutter@imperial.ac.uk) or M.M. (m.merkx@tue.nl).

Author contributions

J.L.V., G.A.R and M.M. designed research; J.L.V., T.J.N., E.A.B., M.S.K. conducted experiments, J.L.V., T.J.R., E.A.B, M.S.K., G.A.R. and M.M. analyzed data, and J.L.V., G.A.R. and M.M. wrote the paper.

Europe PMC Funders Author Manuscripts

metallochaperones and metal-regulated transcription factors. The affinities of the latter have been used to argue that the free concentration of Zn^{2+} in *E. coli* should be ~1 fM8, while the concentration of free Cu^{+} in yeast was estimated to be 10^{-18} M2. In order to progress our understanding of transition metal homeostasis and its involvement in diseases, tools are required that allow direct (sub)cellular imaging of transition metal concentrations in single living cells in real time. In recent years an impressive variety of Zn^{2+} sensitive fluorescent dyes (such as Zinquin, rhodzin-3 and FluoZin-3) have been developed, some of which have also been applied to monitor Zn^{2+} fluctuations in living cells9,10. However, synthetic probes come with a few intrinsic limitations, notably a lack of full control over subcellular localization and the need to achieve high intracellular concentrations of the dye which may perturb free levels of Zn^{2+}. In addition, it has proven challenging to create synthetic dyes that rival the affinity and specificity typically observed with metalloproteins, which is important to reliably determine the extremely low concentrations of Zn^{2+} and other transition metal ions4,11,12.

The power of recombinant targeted probes has been well-established in the Ca^{2+} signaling field, using bioluminescent proteins such as aequorin13 or spectrally-shifted variants of GFP engineered to include suitable binding motifs. In particular, the development of Förster Resonance Energy Transfer (FRET)-based sensor proteins has allowed accurate monitoring of Ca^{2+} fluxes, from the subcellular level to entire organisms, and from the subsecond timeframe to a period of weeks14–16. While some progress has been reported in developing similar FRET-based sensor proteins for Zn(II)12,17,18, at present these sensors have not allowed imaging of free Zn^{2+} levels in mammalian cells.

Here we report the development of genetically-encoded sensor proteins that for the first time are capable of accurately and dynamically reporting on the extremely low concentration of Zn^{2+} in the cytosol of single mammalian cells in real time. A new FRET-sensor concept based on conformational switching was introduced to increase the ratiometric response of a previously reported Zn^{2+} sensor by six-fold. The Zn^{2+} affinity of this sensor was then systematically attenuated to yield sensor variants with K_d-values between 2 pM and 3 nM. Using this array of sensors proved essential to accurately measure the concentration of free Zn^{2+} in the cytoplasm of HEK293 cells. Through the incorporation of a suitable targeting sequence into the corresponding cDNAs, these tools were subsequently used to gain specific insights into zinc homeostasis within the cytosol and secretory granule of a specialized secretory cell type, the pancreatic β-cell, where Zn^{2+} is required for insulin storage19 and has been implicated in controlling hormone release20.

Results

A FRET-based Zn^{2+} sensor based on conformational switching

We previously reported the development of a genetically encoded FRET-based Zn^{2+} sensor (CALWY) that consists of two metal binding domains (ATOX1 and WD4) linked via a long flexible peptide linker, with enhanced cyan and yellow fluorescent protein (ECFP and EYFP, respectively) flanking the two metal binding domains (Figure 1a)12. This sensor displayed a very high Zn^{2+} affinity (K_d = 0.23 pM at pH 7.1). However, like many other genetically-encoded FRET sensors this probe displayed only a small ratiometric response, with a ~15 %

decrease in emission ratio upon Zn^{2+} binding (Figure 1b,c). Our analysis showed that this small change was caused by the presence of a distribution of conformations in the Zn^{2+}-free state whose average energy transfer efficiency was only slightly higher than the amount of energy transfer in the Zn^{2+}-bound state12. Recently we demonstrated that introduction of two mutations, S208F and V224L, can promote formation of a weak intramolecular complex between two fluorescent domain present in a single fusion protein resulting in a substantial increase in energy transfer efficiency21. Following replacement of ECFP and EYFP by Cerulean and Citrine, the same mutations were introduced in the CALWY sensor yielding enhanced CALWY-1 (eCALWY-1). This variant indeed displayed a much higher emission ratio, and thus much more efficient energy transfer, in the unbound state (Figure 1d-f). Addition of Zn^{2+} resulted in a two-fold decrease in emission ratio, representing an improvement of the dynamic range of the sensor output of 600%. Importantly, the Zn^{2+} affinity of eCALWY-1 (K_d = 2 pM at pH 7.1) was only 10-fold lower than that of the wild-type sensor, showing that the intramolecular interaction between the fluorescent domains was subtle and easily disrupted by Zn^{2+} binding. Independent evidence for the proposed conformational switching mechanism depicted in Figure 1d was obtained from fluorescence anisotropy measurements that showed an increase in rotational tumbling of the Citrine domain upon Zn^{2+} binding (Supplementary Methods, Figure S4).

To test whether eCALWY-1 was able to detect changes in free cytosolic Zn^{2+} levels, we monitored the Cerulean and Citrine emission in single HEK293 fibroblasts using fluorescence microscopy. A two-fold increase in emission ratio was observed after perifusion with 50 μM of the membrane permeable zinc chelator N,N,N',N'-tetrakis-(2-pyridylmethyl)-ethylenediamine (TPEN) for cells expressing eCALWY-1 (Figure 1g,h), consistent with a decrease in the cytosolic free Zn^{2+} concentration. Subsequent perifusion with 5 μM of the zinc ionophore pyrithione had a minor effect, but exposure of the cells to 100 μM $ZnCl_2$ and 5 μM pyrithione resulted in a strong decrease in emission ratio. Since the emission ratio obtained after saturation with Zn^{2+} was identical to the ratio at the start of the experiment, we concluded that eCALWY-1 was already fully saturated in cells under the normal culture conditions. No changes in emission ratio were observed when TPEN or zinc and pyrithione were added to cells expressing a non-binding variant of eCALWY that lacked the metal-binding cysteines, confirming that Zn^{2+} binding was responsible for the changes observed for eCALWY-1 (Figure 1g).

Determination of free Zn^{2+} levels using a toolbox of zinc sensors

Since the eCALWY-1 sensor was shown to be saturated with Zn^{2+} in HEK293 cells under normal culture conditions, we next developed a series of weaker eCALWY variants covering a range of Zn^{2+} concentrations. Two complementary strategies were employed to systematically tune the Zn^{2+} affinity of eCALWY-1. A single cysteine-to-serine mutation in the metal binding site of the WD4 domain was found to attenuate the Zn^{2+} affinity 300-fold, yielding the eCALWY-4 sensor with a K_d of 600 pM. Further fine-tuning of the Zn^{2+} affinity was achieved by shortening the flexible peptide linker between the metal binding domains of eCALWY-1 and eCALWY-4 from 9 to either 5 (eCALWY-2 and eCALWY-5) or 3 GGSGGS repeats (eCALWY2 and eCALWY-6). As reported previously for the original CALWY sensors, shortening of the peptide linker resulted in 3-10 fold lower Zn^{2+} affinities (Table 1,

Figure 2a)12. All sensor variants displayed a two-fold change in emission ratio, while their K_d's together spanned three orders of magnitude.

Figures 2b-g show the responses of all six eCALWY variants transiently expressed in HEK293 cells to a protocol of TPEN addition followed by Zn^{2+}/pyrithione treatment (see also Video S1). The responses observed for each sensor correlate well with their *in vitro* determined K_d. The emission ratio at the start of experiment showed a consistent trend changing from the Zn^{2+}-saturated level for eCALWY-1 to the Zn^{2+}-depleted level for eCALWY-6. A substantially faster equilibration upon TPEN addition was observed for the weaker sensor variants, probably reflecting an increase in Zn^{2+} dissociation rate caused by the C416S mutation. The occupancy of the sensor at the start of the experiment was calculated using equation 1, in which R_{max} and R_{min} are the steady-state ratios obtained after TPEN and zinc/pyrithione addition, respectively, and R_{start} is the ratio at the start of the experiment.

$$Occupancy = \frac{R_{max} - R_{start}}{R_{max} - R_{min}} \cdot 100\% \quad (1)$$

A plot of the sensor occupancy as a function of its K_d shows a clear sigmoidal shape, that is best described by assuming a free Zn^{2+} concentration of ~400 pM (Figure 2h). The plot also shows the predicted occupancies assuming different values of free Zn^{2+} and illustrates that the free Zn^{2+} concentration in HEK293 cells is buffered between 200 and 800 pM. Importantly, the fact that the occupancies of the entire sensor series can be described by a single concentration of free Zn^{2+} suggests that the intracellular free Zn^{2+} concentration is not significantly disturbed by the presence of the sensor.

Cytosolic Zn^{2+} homeostasis in pancreatic β-cells

Insulin-containing secretory vesicles present in pancreatic β-cells are known to store tens of millimolar concentrations of Zn^{2+} ions5 which are required to store insulin in a hexameric form19. To test whether Zn^{2+} transport into secretory vesicles would lower the steady-state cytosolic Zn^{2+} levels, we determined free Zn^{2+} in clonal rat pancreatic β-cells (INS-1(832/13)) cells22 using the same approach as described above for HEK293 cells. The responses of the various sensor variants in INS-1(832/13) cells, which contain abundant secretory vesicles, were found to be very similar to those in HEK293 cells. A plot of sensor occupancy versus sensor K_d's yielded again a free Zn^{2+} concentration of ~400 pM, suggesting that this value may be relatively invariable among different mammalian cell types (Figure 3a).

The determination of intracellular free Zn^{2+} concentration assumes that the Zn^{2+} affinity of the sensor in the cell is similar to that of the purified protein studied *in vitro*. To verify whether the Zn^{2+} affinity of eCALWY was affected by intracellular conditions such as macromolecular crowding or interactions with endogenous proteins, an intracellular calibration was performed in clonal INS-1(832/13) cells expressing eCALWY-4. Cells were permeabilized for 30 s using *S. aureas* α-toxin to create 3 kDa sized pores that allow free ion

exchange between buffer and cytosol, but prevent proteins from leaking out.23 Subsequently, cells were perifused with a buffer containing physiologically relevant free magnesium and calcium ion levels (0.35 mM and 100 nM, respectively) and different concentrations of free zinc ions (Figure 3b). In each experiment, cells were exposed to two different concentrations of free Zn^{2+}, followed by excess EDTA and excess $ZnCl_2$. Using the latter two conditions to determine the minimum and maximum emission ratios, the occupancy of the eCALWY-4 sensor was calculated at four different free zinc concentrations using equation 1. Although a plot of the sensor occupancy as a function of free Zn^{2+} concentration suggest a slightly lower intracellular K_d of 100-200 pM (Figure 3c), this calibration nonetheless confirms that the Zn(II) affinity of eCALWY-4 is not significantly affected by the intracellular environment.

We next determined whether cytosolic free Zn(II) concentrations may change during the stimulation of β cells with secretagogues since it is conceivable that Zn^{2+} co-released with insulin may re-enter the cells via Zn^{2+} uptake mechanisms (including members of the zinc importer, ZiP family)3. Free cytosolic Ca^{2+} concentrations in β-cells increase from ~100 nM to ~500 nM or ~1 μM upon stimulation with elevated glucose or KCl concentrations, respectively, due to plasma membrane depolarization (caused by the closure of ATP-sensitive K^+ channels in the case of glucose) and the opening of voltage-sensitive Ca^{2+} channels24. No changes in the free Zn^{2+} concentration were observed upon addition of 20 mM glucose (not shown) or 25 mM KCl (Figure 3d) to INS-1(832/13) cells expressing the eCALWY-4 sensor that had been starved overnight with 3 mM glucose, however. The KCl responsiveness of the cells was confirmed when the same experiment was performed with cells expressing eCALWY-4 and loaded with the Ca^{2+} dye Fluo-3, as shown by the expected spike and oscillations in calcium levels (Figure S7). These observations suggest that cytosolic Zn^{2+} levels are not easily disturbed by external stimuli or by large changes in the concentrations of other divalent metal ions including Ca^{2+}.

Vesicular targeting of Zn^{2+} probes

An important advantage of the use of genetically-encoded probes for measuring intracellular ion concentrations is the capacity to address these probes to specific intracellular domains through the incorporation of specific targeting motifs13,15,24,25. Having established the potency of the eCALWY sensors to probe Zn^{2+} concentrations in the cytosol, we next explored whether these probes could be targeted to other intracellular organelles with a potentially important role in Zn^{2+} homeostasis. Sensors targeted to insulin-containing granules of β-cells were generated by fusion to the C-terminus of the vesicle associated membrane protein 2 (VAMP2), a protein previously used to target aequorin to the granule matrix in β-cells (Figure 4a)25. Colocalization studies with a granule-localised neuropeptide Y-mCherry fusion protein26 by confocal microscopy showed that VAMP2-eCALWY-1 and VAMP2-eCALWY-6 proteins were indeed exclusively localized to insulin-containing granules (Figure 4b; Figure S10). Both VAMP2-eCALWY-1 and VAMP2-eCALWY-6 showed a low emission ratio, suggesting that both were fully saturated at ambient intragranular Zn^{2+} concentrations (Figure 4c,d). The emission ratio of VAMP2-eCALWY-1 did not respond to the addition of either TPEN or $ZnCl_2$ and pyrithione, however. While this could mean that the eCALWY sensors were not functional when targeted to granules, it is

more likely that insufficient TPEN was able to cross the granular membrane to significantly lower the granular free Zn^{2+} concentration. To test this hypothesis, we targeted another genetically-encoded Zn^{2+} sensor, eZinCh-1, to the granules as a VAMP2 fusion protein. This previously reported sensor has a relatively weak Zn^{2+} affinity (K_d = 1 μM at pH 7.1 and 250 μM at pH 6.0; Supplementary Fig, S8), but displays a four-fold increase in emission ratio upon Zn^{2+} binding *in vitro*17. Again, no changes in emission ratio were observed upon perifusion with TPEN or zinc and pyrithione (Figure 4c), but a large ratiometric increase was observed after the addition of monensin (Figure 4d; supplementary video S2). Monensin is a known Na^+/H^+ exchanger that increases the pH of granules from ~ pH 6.0 to cytosolic levels (~pH 7.1)25. This increase in pH is expected not only to increase the Zn^{2+} affinity of eZinCh, but also to release Zn^{2+} ions by the dissolution of the insulin/Zn^{2+} complexes27. TPEN addition after the monensin treatment had no further effect, confirming that TPEN is not able to significantly reduce granular free Zn^{2+} levels (data not shown). From these results, we conclude that the eCALWY sensors are most likely saturated with Zn^{2+} within dense core vesicles under normal conditions, whereas the eZinCh-1 sensor is mostly Zn^{2+}-free. These data therefore suggest that the free Zn^{2+} concentration in the vesicles lies between 1 and 100 μM based on the *in vitro*-determined affinities of these sensors at pH 6.0 (Figure S8 and S9).

Discussion

The genetically-encoded sensors reported here offer several key advantages compared to the synthetic fluorescent dyes that are typically used for studying cellular Zn^{2+} homeostasis: (1) control over subcellular localization and the absence of leakage; (2) a relatively large ratiometric response that is independent of sensor concentration; (3) a high and tunable affinity covering a range between 10^{-9} and 10^{-12} M, and (4) ready delivery to cells by simple transfection protocols. Moreover, our results suggest that promoting intramolecular domain interactions could be a generic, rational design strategy to improve the dynamic response of FRET-based sensors, which is an important prerequisite to extent their application to high throughput methods such as fluorescence activated cell sorting (FACS)28.

The availability of sensors covering a range of Zn^{2+} affinities proved critical to reliably determine the cytosolic Zn^{2+} concentration. An important potential problem with measuring intracellular metal concentrations is that the presence of the sensor perturbs the free metal concentration. This is particularly true in this case where the free metal concentration of ~400 pM (corresponding to ~100 free Zn^{2+} ions per cell) is 10^3-10^4 fold lower than that of the sensor protein. Two observations indicate that the free Zn^{2+} concentration was not significantly affected, however. First, the occupancies of the sensor proteins were found to be independent of the expression level. More importantly, the occupancies of all six eCALWY variants were well described by their K_d values and a single free Zn^{2+} concentration. If the sensors had perturbed the free Zn^{2+} concentration substantially one would expect lower occupancies for the high affinity sensors than observed here.

The free Zn^{2+} concentration of ~400 pM reported here is similar to the 600 pM that was recently reported by Maret and coworkers using the fluorescent dye FluoZin-34. However, its relatively low affinity for Zn^{2+} (K_d = 15 nM) renders FluoZin-3 suboptimal for

measuring subnanomolar concentrations. In addition, this probe probably does not exclusively report the cytosolic Zn^{2+} concentration, having a strong tendency to accumulate in intracellular organelles including secretory vesicles (GAR, unpublished observations). Using a sensor based on fluorescently-labeled carbonic anhydrase11, Bozyme *et al* reported a significantly lower free Zn^{2+} concentration of 5 pM in PC12 cells by comparing the absolute emission ratio measured in the cell directly to an *in vitro* calibration curve. We observed significant variability in the absolute emission ratio among cells that expressed the same fluorescent sensor, however, probably as a result of variation in the contribution of background fluorescence. In our hands, reliable estimation of the free Zn^{2+} concentration therefore always required measurement of the emission ratios corresponding to 0 % and 100 % sensor occupancy.

The observation that the cytosolic free Zn^{2+} concentration is similar in two substantially different mammalian cell types (fibroblastic and secretory), suggests that cytosolic Zn^{2+} levels are carefully controlled and might not vary much between different mammalian cell types. Moreover, the demonstration that cytosolic free Zn^{2+} concentrations did not change in β-cells under conditions in which cytosolic Ca^{2+} concentrations fluctuated considerably provides evidence both for the selectivity of the reporters *in situ*, and for the view that the concentrations of these two metal ion species can be regulated entirely independently. Maret and coworkers29 recently showed that metallothioneines can provide robust Zn^{2+} buffering in the range between 10^{-11} and 10^{-9} M, which nicely coincides with the ~400 pM of free Zn^{2+} obtained in this study. Intriguingly, cytosolic Zn^{2+} concentrations are thus maintained at a level that is sufficient to fully saturate native Zn^{2+} proteins (which typically show K_d's of 1-10 pM)30, but approximately 10-fold below the low nM concentrations that have been reported to be inhibitory to certain cytosolic proteins.

In conclusion, we have developed a new generation of Zn^{2+} probes that, delivered using simple plasmid transfection protocols, can be used as a convenient means of detecting and imaging low cytosolic free Zn^{2+} concentrations dynamically and in real time in living cells. Importantly, we demonstrate that these probes are molecularly targetable to subcellular organelles, including the secretory granule. The availability of this new sensor toolbox is expected to allow much more detailed studies of Zn^{2+} homeostasis in a variety of organelles and a wide range of cell types, including the identification of new proteins involved in maintaining Zn^{2+} homeostasis and the possibility to more directly assess the role of transition metal homeostasis in health and disease3.

Methods

Intracellular FRET imaging

Cells were imaged by using an Olympus IX-70 (Melville, NY) microscope fitted with a monochromator (Polychrome IV, TILL Photonics, Grafelfing, Germany) and a MAGO charge-coupled device camera (TILL Photonics) controlled by TILLVISION software (TILL Photonics). For FRET measurements, a 455DRLP dichroic mirror (Chroma Technology, Brattleboro, NY) and two emission filters (D465/30 for Cerulean and D535/30 (Chroma) for Citrine) alternated by a filter changer (Lambda 10–2, Sutter Instruments, San Rafael, CA)

were used. Images were acquired at 1 Hz using a 100 ms exposure time and a 433 nm excitation wavelength.

Cells were imaged in modified Krebs–Hepes/bicarbonate (KB) buffer, consisting of 132.5 mM NaCl, 3.6 mM KCl, 0.5 mM NaH_2PO_4, 0.5 mM $MgSO_4$, 1.5 mM $CaCl_2$, 10 mM Hepes, 2 mM $NaHCO_3$ and 3 mM glucose and was then preequilibrated with 95:5 O_2:CO_2, pH 7.4. TPEN and pyrithione were prepared fresh on the day of use in 25 mM and 1 mM stock solutions in DMSO, respectively. Buffers were added using perifusion (2 mL/min) with KB plus additions as stated (37 ºC). Where indicated, cells were permeabilized by adding 20 µl of 250 µg/ml α-toxin dissolved in intracellular buffer (IB) to 100 µl of INS-1(832/13) cells in IB. IB comprised 140 mM KCl, 10 mM KH_2PO_4 2 mM $MgSO_4$, 1 mM ATP, 2 mM Na^+ succinate, 20 mM Hepes, and 5.5 mM glucose and was then pre-equilibrated with 95:5 O_2:CO_2, pH 7.05. After 30 s of incubation with α-toxin, perifusion was used to incubate the cells in fresh IB (2 mL/min). Next, cells were exposed to IB containing different amounts of Ca^{2+}, Mg^{2+}, Zn^{2+} that were buffered using combinations of EGTA and EDTA or HEDTA (Table S4).

Supplementary Material

Refer to Web version on PubMed Central for supplementary material.

Acknowledgements

We thank S.M.J. van Duijnhoven for the expression and characterization of eZinCh-1, Dr. A. McDonald for assisting in the co-localization studies, Dr. A. Tarasov for setting up the α-toxin incubation, Prof. H. Bayley (University of Oxford) for kindly providing the α-toxin and Dr Chris Newgard (Duke University) for the provision of INS-1(832/13) cells. We also thank Dr L. Klomp and P. van den Berghe (University Medical Center Utrecht) for their support in early stages of this research. MM and MSK acknowledge support by the Human Frontier of Science Program (HPSF Young Investigator Grant, (RGY)0068-2006). GAR thanks the National Institutes of Health for Project grant RO1 DK071962-01, the Wellcome Trust for Programme grants 067081/Z/02/Z and 081958/Z/07/Z, the MRC (UK) for Research Grant G0401641, and the EU FP6 (“SaveBeta” consortium grant). TJN and EAB were supported by Imperial College Divisional Studentships.

Literature

1. Valko M, Morris H, Cronin MT. Metals, toxicity and oxidative stress. Curr Med Chem. 2005; 12:1161–1208. [PubMed: 15892631]
2. Rae TD, Schmidt PJ, Pufahl RA, Culotta VC, O'Halloran TV. Undetectable intracellular free copper: the requirement of a copper chaperone for superoxide dismutase. Science. 1999; 284:805–808. [PubMed: 10221913]
3. Cousins RJ, Liuzzi JP, Lichten LA. Mammalian zinc transport, trafficking, and signals. J Biol Chem. 2006; 281:24085–24089. [PubMed: 16793761]
4. Krezel A, Maret W. Zinc-buffering capacity of a eukaryotic cell at physiological pZn. J Biol Inorg Chem. 2006; 11:1049–1062. [PubMed: 16924557]
5. Hutton JC, Penn EJ, Peshavaria M. Low-molecular weight constituents of isolated insuline-secretory granules- bivalent-cations, adenine-nucleotides and inorganic phosphates. Biochem J. 1983; 210:297–305. [PubMed: 6344863]
6. Linkous DH, et al. Evidence hat the ZnT3 protein controls the total amount of elemental zinc in synaptic vesicles. J Histochem Cytochem. 2008; 56:3–6. [PubMed: 17712179]
7. Ho LH, et al. Labile zinc and zinc transporter ZnT4 in mast cell granules: Role in regulation NF-KB translocation. J Immunology. 2004; 172 77507760.

8. Outten CE, O'Halloran TV. Femtomolar sensitivity of metalloregulatory proteins controlling zinc homeostasis. Science. 2001; 292:2488. [PubMed: 11397910]
9. Domaille DW, Que EL, Chang CJ. Synthetic fluorescent sensors for studying the cell biology of metals. Nat Chem Biol. 2008; 4:168–175. [PubMed: 18277978]
10. Nolan EM, Lippard SJ. Small-molecule fluorescent sensors for investigating zinc metalloneurochemistry. Acc Chem Res. 2009; 42:193–203. [PubMed: 18989940]
11. Bozym RA, Thompson RB, Stoddard AK, Fierke CA. Measuring picomolar intracellular exchangeable zinc in PC-12 cells using a ratiometric fluorescence biosensor. ACS Chem Biol. 2006; 1:103–111. [PubMed: 17163650]
12. van Dongen EMWM, et al. Variation of linker length in ratiometric fluorescent sensor proteins allows rational tuning of Zn(II) affinity in the picomolar to femtomolar range. J Am Chem Soc. 2007; 129:3494–3495. [PubMed: 17335212]
13. Rizzuto R, Simpson AWM, Brini M, Pozzan T. Rapid changes of mitochrondrial Ca^{2+} revealed by specifically targeted recombinant aequorin. Nature. 1992; 358:325–327. [PubMed: 1322496]
14. Mank M, et al. A genetically encoded calcium indicator for chronic in vivo two-photon imaging. Nat Methods. 2008; 5:805–811. [PubMed: 19160515]
15. Miyawaki A, et al. Fluorescent indicators for Ca^{2+} based on green fluorescent proteins and calmodulin. Nature. 1997; 388:882–887. [PubMed: 9278050]
16. Wallace DJ, et al. Single-spike detection in vitro and in vivo with a genetic Ca^{2+} sensor. Nat Methods. 2008; 5:797–804. [PubMed: 19160514]
17. Evers TH, Appelhof MAM, de Graaf-Heuvelmans PTHM, Meijer EW, Merkx M. Ratiometric detection of Zn(II) using chelating fluorescent protein chimeras. J Mol Biol. 2007; 374:411–425. [PubMed: 17936298]
18. Qiao W, Mooney M, Bird AJ, Winge DR, Eide DJ. Zinc binding to a regulatory zinc-sensing domain monitored in vivo by using FRET. Proc Natl Acad Sci USA. 2006; 103:8674–8679. [PubMed: 16720702]
19. Dodson G, Steiner D. The role of assembly in insulin's biosynthesis. Curr Opin Struct Biol. 1998; 8:189–194. [PubMed: 9631292]
20. Sladek R, et al. A genome-wide association study identifies novel risk loci for type 2 diabetes. Nature. 2007; 445:881–885. [PubMed: 17293876]
21. Vinkenborg JL, Evers TH, Reulen SW, Meijer EW, Merkx M. Enhanced sensitivity of FRET-based protease sensors by redesign of the GFP dimerization interface. ChemBioChem. 2007; 8:1119–1121. [PubMed: 17525917]
22. Hohmeier HE, et al. Isolation of INS-1-erived cell lines with robust ATP-sensitive K+ channel-dependent and independent glucose-stimulated insulin secretion. Diabetes. 2000; 49:424–430. [PubMed: 10868964]
23. Tarasov AI, Girard CA, Ashcroft FM. ATP sensitivity of the ATP-sensitive K^+ channel in intact and permeabilized pancreatic beta-cells. Diabetes. 2006; 55:2446–2454. [PubMed: 16936192]
24. Rutter GA, et al. Stimulated Ca^{2+} influx raises mitochrondrial free Ca^{2+} to supramicromolar levels in a pancreatic beta-cell line. Possible role in glucose and agonist-induced insuline secretion. J Biol Chem. 1993; 268:22385–22390. [PubMed: 8226749]
25. Mitchell KJ, et al. Dense core secretory vesicles revealed as a dynamic Ca(2+) store in neuroendocrine cells with a vesicle-associated membrane protein aequorin chimera. J Cell Biol. 2001; 155:41–51. [PubMed: 11571310]
26. Tsuboi T, Rutter GA. Multiple forms of "kiss-and-run" exocytosis revealed by evanescent wave microscopy. Curr Biol. 2003; 13:563–567. [PubMed: 12676086]
27. Hutton JC. The internal pH and membrane potential of the insulin-secretory granule. Biochem J. 1982; 204:171–178. [PubMed: 6126183]
28. Ouyang M, Sun J, Chien S, Wang Y. Determination of hierarchical relationship of Src and Rac at subcellular locations with FRET biosensors. Proc Natl Acad Sci USA. 2008; 105:14353–14358. [PubMed: 18799748]
29. Krezel A, Maret W. Dual nanomolar and picomolar Zn(II) binding properties of metallothionein. J Am Chem Soc. 2007; 129:10911–10921. [PubMed: 17696343]

30. Krezel A, Maret W. Thionein/metallothionein control Zn(II) availability and the activity of enzymes. J Biol Inorg Chem. 2008; 13:401–409. [PubMed: 18074158]

Europe PMC Funders Author Manuscripts

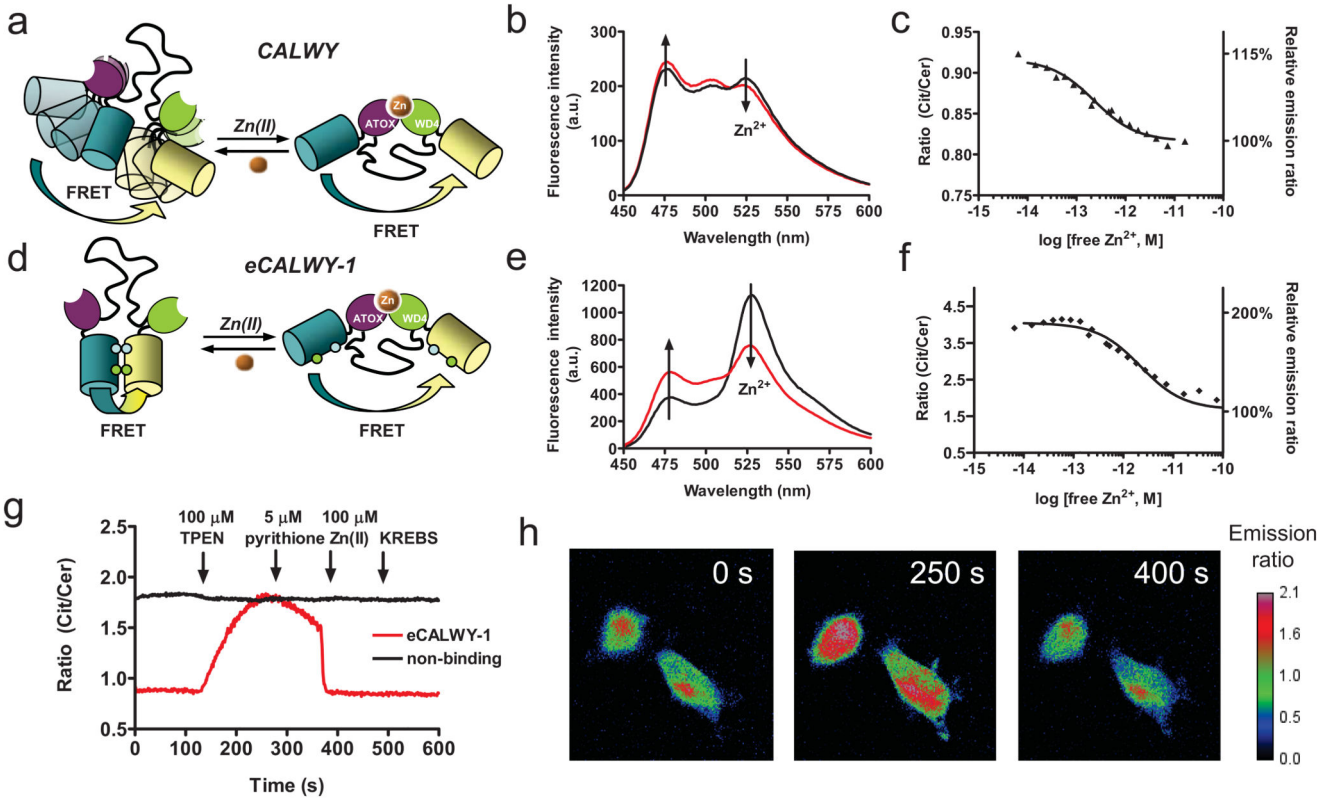

Figure 1. Design and properties of eCALWY-1, a genetically-encoded Zn^{2+} sensor based on conformational switching.

Schematic representation of the CALWY (a) and eCALWY-1 (b) sensors. Introduction of S208F and V224L mutations fluorescent domains results in large increase in the ratiometric response. Emission spectra of CALWY (c) and eCALWY-1 (d) before (black line) and after (red line) addition of 0.9 mM Zn^{2+} in 1 mM HEDTA (b) or EGTA (e). Zn^{2+} titrations of CALWY (c) and eCALWY-1 (f), showing the ratio of yellow and cyan emission (R527/475) as a function of Zn^{2+} concentration using 420 nm excitation. The solid lines depict fits assuming single binding events with K_d's of 0.22 and 2 pM for CALWY and eCALWY-1, respectively. Measurements were performed using ~ 1 μM protein in 150 mM Hepes, 100 mM NaCl, 10% (v/v) glycerol, pH 7.1 at 20 ºC. (g) Response of single HEK293 cells expressing either eCALWY-1 or a non-binding variant (eCALWY-NB) to Zn^{2+} depletion and addition as measured by the ratio of Citrine and Cerulean emission. Cells were perfused with KB buffer (0 s), KB buffer containing 50 μM TPEN (120 s), 5 μM pyrithione (240 s), 5 μM pyrithione/100 μM Zn(II) (360 s) and KB buffer (480 s). (h) False-colored fluorescence ratio micrographs of HEK293 cells expressing eCALWY-1 after 0, 250, and 400 s of the experiment described in (g).

Europe PMC Funders Author Manuscripts

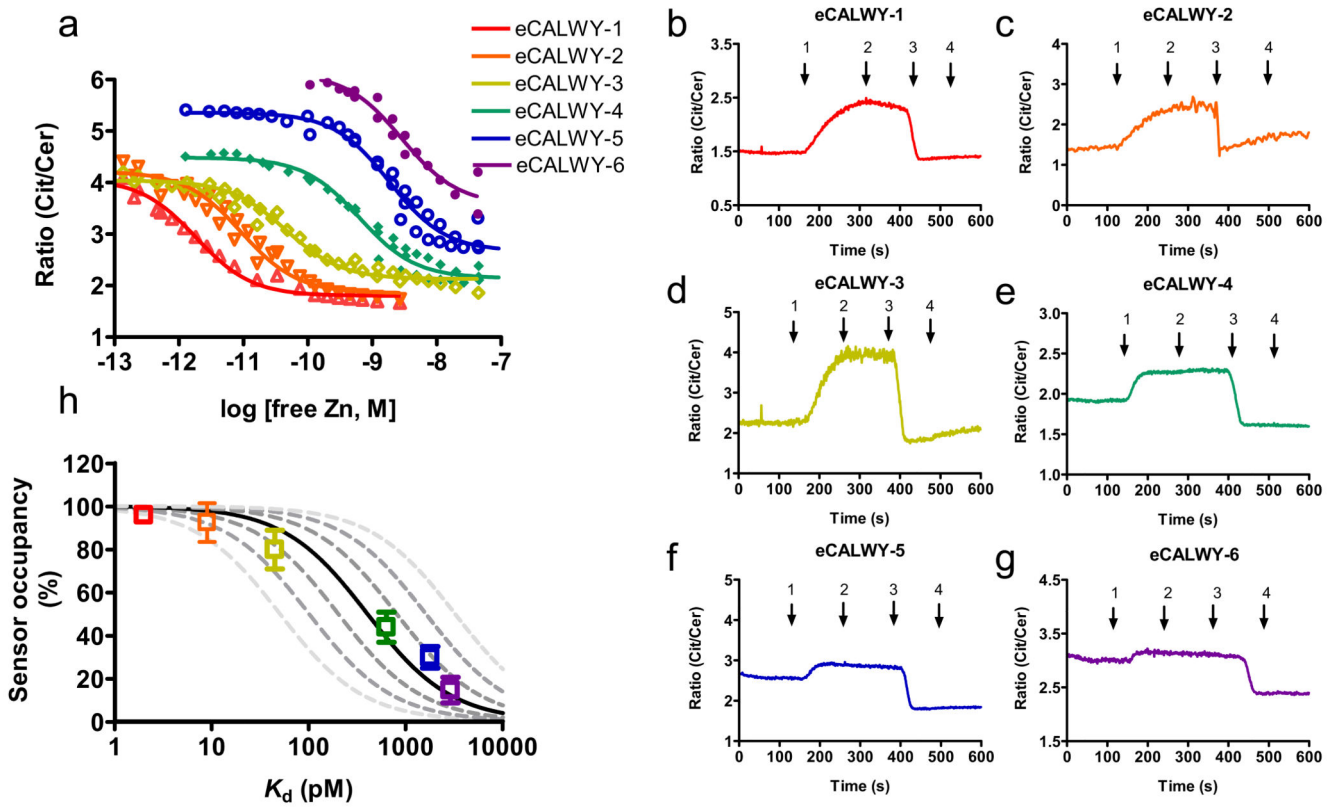

Figure 2. Determination of cytosolic free Zn^{2+} concentration in HEK293 cells using a toolbox of eCALWY variants.

(a) Citrine over Cerulean emission ratio versus free zinc concentration for the different eCALWY variants. Solid lines represent fits assuming a single binding event with the K_d's listed in Table 1. (b-g) Responses of single HEK293 cells expressing eCALWY-1-6 to a protocol of KREBS buffer with 50 μM TPEN (1), 5 μM pyrithione (2), 5 μM pyrithione/100 μM Zn(II) (3) or no additives (4). (h) Sensor occupancy in HEK293 cells as a function of the sensor K_d. Datapoints show the occupancy of the different eCALWY variants as determined from the traces in Supplementary Figure S5 using equation 1, error bars indicate the standard deviation. The solid line represents the expected response to a free cytosolic zinc concentration of 400 pM. The dashed lines depict the expected responses assuming free zinc concentrations of 50, 100, 200, 800, 1600, and 3200 pM, respectively.

Europe PMC Funders Author Manuscripts

Europe PMC Funders Author Manuscripts

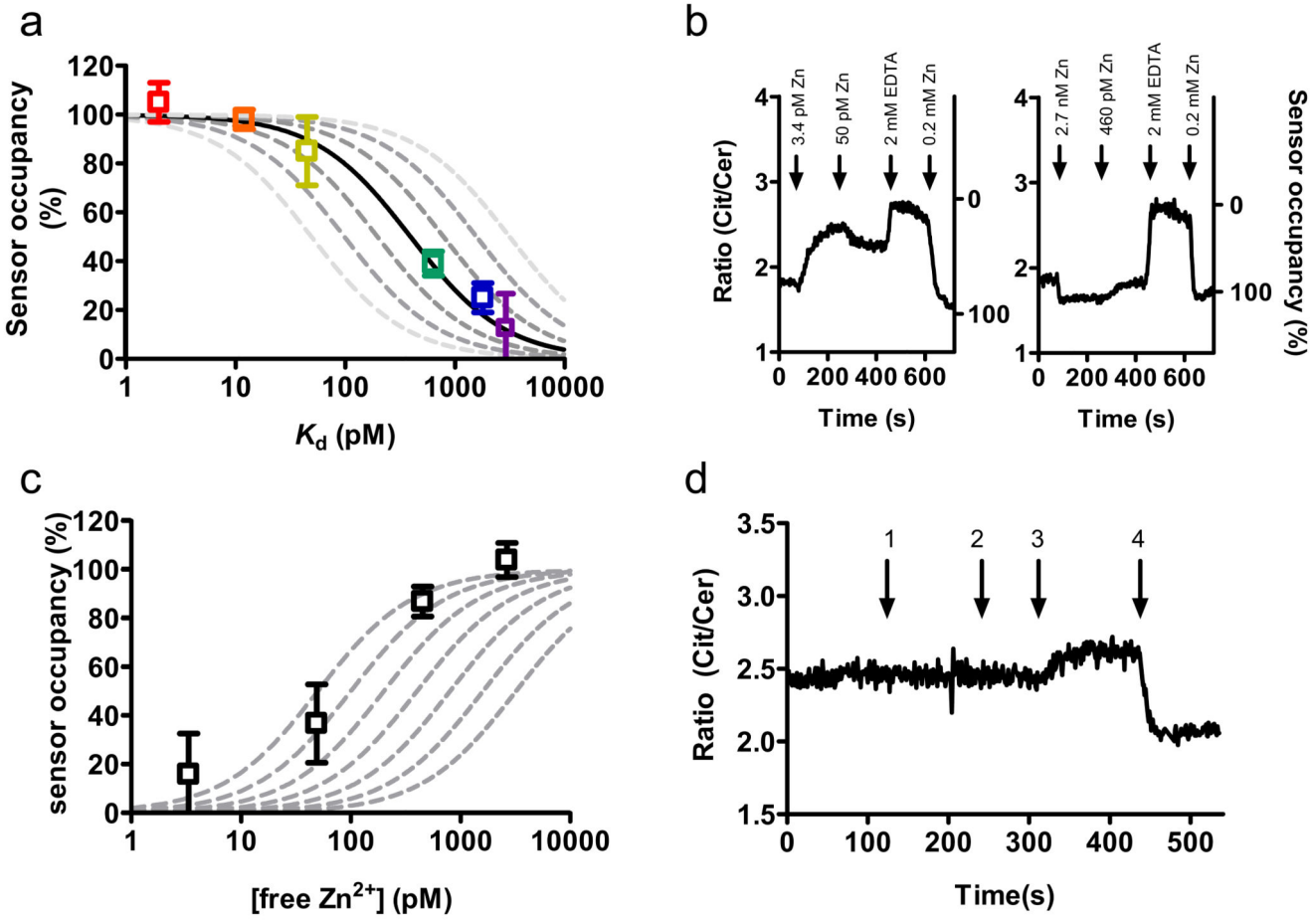

Figure 3. Monitoring cytosolic free Zn^{2+} concentration in pancreatic β-cells.

(a) Sensor occupancy in INS-1(832/13) cells as a function of the sensor K_d. Datapoints show the occupancy of the different eCALWY variants as determined from the traces in Supplementary Figure S6 using equation 1. The solid line represents the expected response to a free cytosolic zinc concentration of 400 pM. The dashed lines depict the expected responses assuming free zinc concentrations of 50, 100, 200, 800, 1600, and 3200 pM, respectively. (b) Citrine over Cerulean emission ratio of a permeabilized INS-1(832/13) cell expressing eCALWY-4 perfused with intracellular buffer containing various amounts of free zinc, followed by perifusion with 2 mM EDTA and 0.2 mM Zn(II). (c) Occupancy of the eCALWY-4 sensor as a function of the free zinc concentration in permeabilized INS-19832/13. The dashed lines show the expected responses for K_d values of 50, 100, 200, 400, 800, 1600 and 3200 pM, respectively. (d) Ratiometric response of an INS-1(832/13) cell expressing eCALWY-4 upon perifusion with KREBS buffer with 25 mM KCl (1), regular KREBS (2), 50 μM TPEN (3) and 5 μM pyrithione/100 μM Zn^{2+} (4).

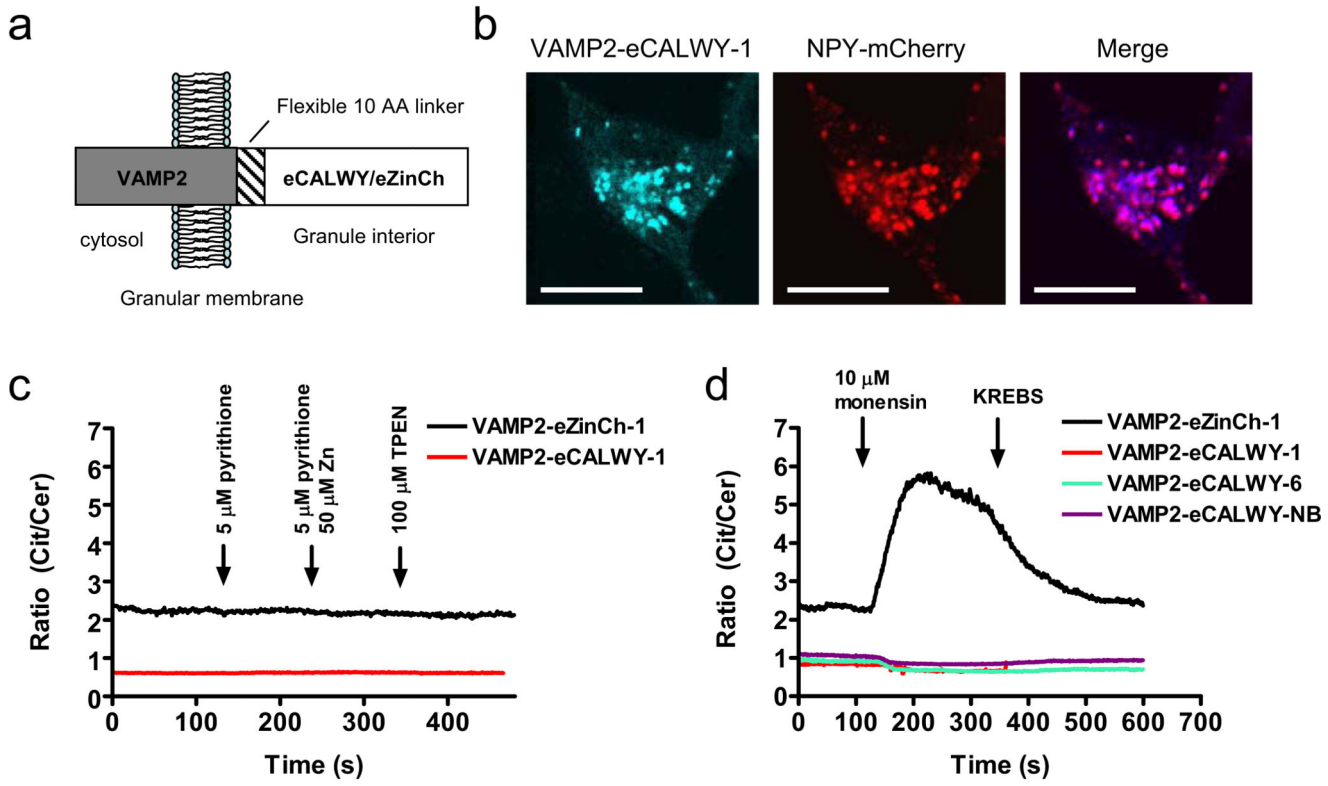

Figure 4. Subcellular targeting of Zn^{2+} probes to insulin-storing granules.

(a) Scheme showing the structural orientation of VAMP2-eCALWY and VAMP2-eZinCh-1 with respect to the granular membrane. (b) Confocal laser scanning microscopy (CLSM) images of INS-1(832/13) cells cotransfected with VAMP2-eCALWY-1 and NPY-mCherry. The VAMP2-eCALWY-1 emission was obtained using excitation at 420 nm, while excitation at 595 nm was used to image NPY-mCherry. The scale bar represents 10 μm. (c) Ratiometric response of INS-1(832/13) cells expressing VAMP2-eZinCh-1 (black line) or VAMP2-eCALWY-1 (red line) to perifusion with 5 μM pyrithione (120 s), 50 μM Zn(II)/ 5 μM pyrithione (240 s) and 100 μM TPEN (360 s), all in KB medium. (d) Ratiometric response of INS-1(832/13) cells expressing different VAMP2-eCALWY variants or VAMP2-eZinCh-1 to perifusion with 10 μM monensin (120 s), followed by regular KB buffer (240 s).

Europe PMC Funders Author Manuscripts

Europe PMC Funders Author Manuscripts

Table 1

Sensor properties of eCALWY variants.

Variant	Number of GGGSGGS repeats in linker	Mutation[a]	Ratiometric change (%)[b]	K_d (Zn^{2+}) (pM)[c]
eCALWY-1	9	-	230	1.8 ± 0.5
eCALWY-2	5	-	230	9 ± 3
eCALWY-3	3	-	190	45 ± 11
eCALWY-4	9	C416S	210	630 ± 160
eCALWY-5	5	C416S	200	1850 ± 600
eCALWY-6	3	C416S	170	2900 ± 1000

[a] The numbering refers to that of the eCALWY sequence. This mutation involves the 2nd cysteine in the MTCXXC motif of the WD4 domain.

[b] Ratiometric change is defined as the emission ratio in the absence of Zn^{2+} divided by the emission ration in the Zn^{2+} bound state.

[c] K_d values were determined in 150 mM Hepes, 100 mM NaCl, 10% (v/v) glycerol, 1 mM DTT pH 7.1. Errors show the 95% confidence intervals obtained from non-linear fits. More information is available in Supplementary Methods.